frontiers | Frontiers in Marine Science

TYPE Correction
PUBLISHED 05 July 2024
DOI 10.3389/fmars.2024.1388621

OPEN ACCESS

EDITED AND REVIEWED BY
Zhiyu Liu,
Xiamen University, China

*CORRESPONDENCE
Ryo Furue
ryofurue@gmail.com

RECEIVED 20 February 2024
ACCEPTED 27 February 2024
PUBLISHED 05 July 2024

CITATION
Furue R (2024) Corrigendum: A seasonal undercurrent along the northwest coast of Australia. *Front. Mar. Sci.* 11:1388621. doi: 10.3389/fmars.2024.1388621

Corrigendum: A seasonal undercurrent along the northwest coast of Australia

Ryo Furue*

Japan Agency for Marine-Earth Science and Technology (JAMSTEC), Yokohama, Japan

KEYWORDS

eddy-resolving oceanic general circulation model, annual cycle, North West Shelf, eastern boundary, coastal trapped waves

A Corrigendum on

A seasonal undercurrent along the northwest coast of Australia

by Furue R (2022) *Front. Mar. Sci.* 8:806659. doi: 10.3389/fmars.2021.806659

In the published article, there was an error. As described and discussed below, the analytic solutions (A5) and (A7) were incorrect and owing to the error some of the figures were also incorrect. The author apologizes for this error and states that this does not change the scientific conclusions of the article in any way. The original article has been updated.

Correction to equations (A5) and (A7)

Solution (A5) was previously:

$$\phi_j(y,t) = \begin{cases} -G_o(L/\pi)[\cos(\pi y/L)+1]\,e^{\imath(\omega t - l_j y)} & 0 < y < L \\ -2G_o(L/\pi)\,e^{\imath(\omega t - l_j y)} & y < 0, \end{cases} \tag{A5}$$

The corrected solution appears below:

$$\phi_j(y,t) = \begin{cases} \frac{-\alpha G_o}{\alpha^2 - l_j^2}[-\imath(l_j/\alpha)\sin\alpha y + \cos\alpha y + e^{-\imath l_j(y-L)}]e^{\imath\omega t} & 0 < y < L \\ \frac{-\alpha G_o}{\alpha^2 - l_j^2}(1 + e^{\imath l_j L})e^{-\imath l_j y}e^{\imath\omega t} & y < 0, \end{cases} \tag{A5}$$

To introduce the new symbol α used in the corrected solution above, the text preceding solution (A5) needs to be modified. It was previously:

$$\tau^y(y,t) = \begin{cases} G_o\sin(\pi y/L)e^{\imath\omega t} & 0 \le y \le L, \\ 0 & \text{otherwise}. \end{cases}$$

The corrected text appears below:

$$\tau^y(y,t) = \begin{cases} G_o(\sin\alpha y)e^{\imath\omega t} & 0 \le y \le L, \\ 0 & \text{otherwise}, \end{cases}$$

where $\alpha \equiv \pi/L$.

As to solution (A7), the relevant text was previously:

and the solution (A5) is modified to

$$\phi_j(y,t) = \begin{cases} -G_o(L/\pi)[\cos(\pi y/L)+1]e^{\imath(\omega t - l_j y)+r' y} & 0 < y < L \\ -2G_o(L/\pi)e^{\imath(\omega t - l_j y)+r'_j y} & y < 0, \end{cases} \quad \text{(A7)}$$

where $r'_j \equiv r_j/c_j$.

The corrected text appears below:

and the solution is identical to (A5) except that $-\imath l_j$ of (A5) is replaced with $-\imath l_j + (r_j/c_j)$ in the present solution.

This change does not affect the rest of the paper because equation number (A7) itself was not referred to anywhere and this was the last equation in the original paper.

Corrected figures

Since the analytic solutions (A5) and (A7) are corrected as described above, all figures plotting the solutions are also corrected. They are Figures 12, 13, A1C, and S7. The corrected figures are all very similar to the original ones and some of them are hardly distinguishable from the original ones.

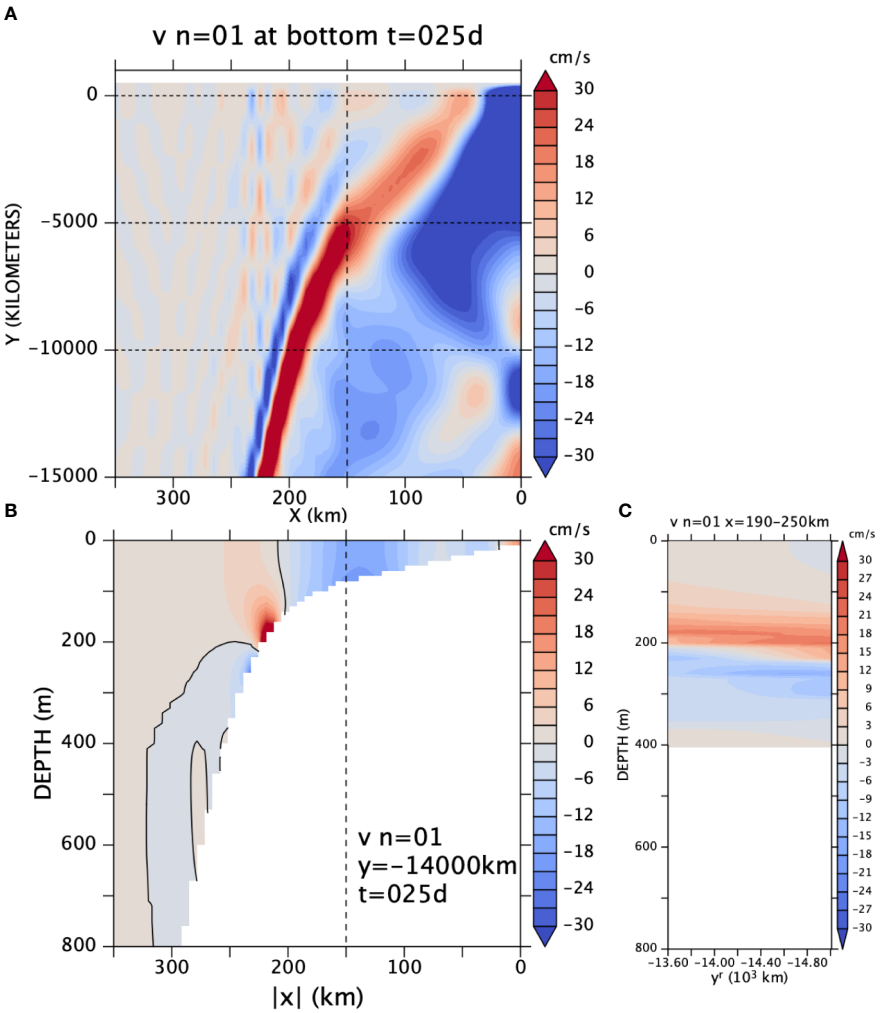

FIGURE 12
v from the CTW model **(A)** along the bottom, **(B)** at y = −14,000 km, and **(C)** averaged over x = 190–250 km at an arbitrary time for the annual frequency. The y-range for **(C)** is the southern-most 1,400 km of **(A)**.

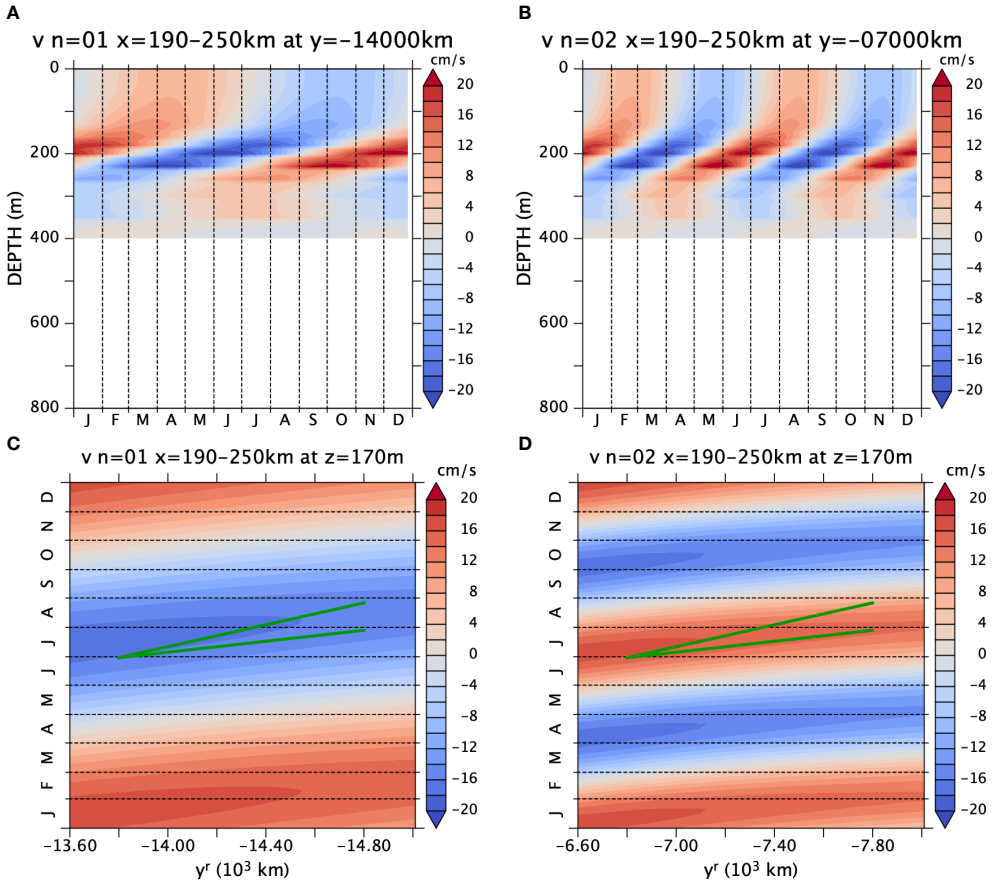

FIGURE 13
v from the CTW model averaged over *x* = 190–250 m **(A)** at *y* = –14,000 km and **(B)** at *y* = –7,000 km; and **(C, D)** at *z* = –170 m **(A, C)** for the annual frequency and **(B, D)** for the semi-annual frequency. The green line segments indicate speeds of 0.2m/s and 0.4m/s. Note that the latitudinal ranges are different between the annual **(A, C)** and semi-annual **(B, D)** frequencies because the beam emerges to the continental slope earlier for the semi-annual frequency. Note also that the range of coloring is narrower (±20 cm/s) here than in Figure 12 because the zonal average weakens the values.

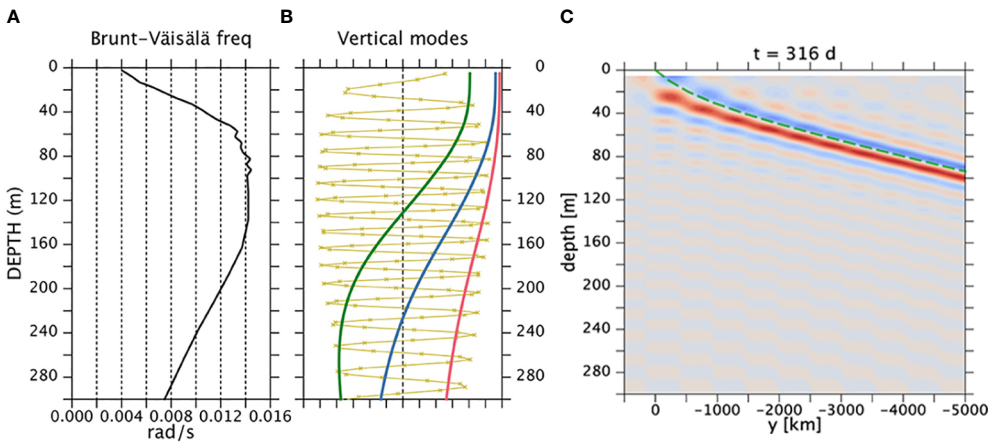

FIGURE A1
(A) Mean Brunt-Väisälä frequency *N(z)* based on WOA13 and **(B)** vertical modes 1, 2, 3, and 100 (red, blue, green, and yellow). The dots on the *j* = 100 mode indicate the gridpoints for the numerical calculation of Equation (4). **(C)** Meridional velocity (snapshot at an arbitrary time and at x = 0, eastern boundary) of coastal Kelvin wave on an f plane forced by an annual wind. The velocity field is constructed as a sum of 100 modes [*j* = 1–100 in formula (1). The total depth is 5,000 m; only the upper 300 m is shown. The green dashed curve is a WKB ray starting from the southern edge of the forcing region (*y* > 0). See text for details.

Publisher's note